

Received February 15, 2017, accepted March 8, 2017, date of publication March 13, 2017, date of current version May 17, 2017.

Digital Object Identifier 10.1109/ACCESS.2017.2681696

Energy Harvesting-Based D2D Communications in the Presence of Interference and Ambient RF Sources

TOAN X. DOAN, TIEP M. HOANG, TRUNG Q. DUONG, (Senior Member, IEEE),
AND HIEN QUOC NGO, (Student Member, IEEE)

Queen's University of Belfast, Belfast BT7 1NN, U.K.

Corresponding author: Trung Q. Duong (trung.q.duong@qub.ac.uk)

This work was supported in part by the U.K. Royal Academy of Engineering Research Fellowship under Grant RF1415n14n22, in part by the U.K. Engineering and Physical Sciences Research Council under Grant EP/P019374/1, and in part by the Newton Institutional Link under Grant ID 172719890.

ABSTRACT This paper considers a device-to-device (D2D) network with time-splitting protocol, where a D2D transmitter (T_x) first harvests energy from a multiple-antenna power beacon (PB) and ambient radio frequency sources, and then uses that harvested energy to transmit data to the D2D receiver (R_x). To improve the energy transfer efficiency, the PB is equipped with multiple antennas for energy transfer, and T_x is equipped with multiple antennas for energy harvesting. Two beamforming techniques, called best antenna-based beamforming and optimal beamforming vector, are proposed to use at the PB. We derive novel analytical expressions for the average harvested energy, power outage probability, and the outage probability of the information transfer link, considering the effect of co-channel interference from homogeneous Poisson distributed interferers and the short-range propagation model for the path loss. We show that by deploying multiple harvesting energy antennas at T_x and by implementing optimal beamforming vector scheme at the PB, the system performance improves substantially. Furthermore, Monte-Carlo simulations are provided and verify the accuracy of our analytical results.

INDEX TERMS D2D communications, interference, energy harvesting, MIMO, stochastic geometry.

I. INTRODUCTION

Interference has been traditionally considered as one of biggest obstacles in wireless networks. Recently, there has been a new trend to exploit the interference to improve the performance of wireless networks, e.g., using the interference as a new mechanism to enhance the security performance [1] or using the interference as an additional source for supplying the power [2]. With unprecedented growth in the volume of wireless data traffic, active time and energy consumption at mobile users are endlessly increasing [3]. Therefore, supplying energy for the mobile users becomes a vital task for next generation wireless systems. A potential candidate that has emerged to deal with this problem is radio frequency wireless power transfer (WPT), due to its ability of transferring energy for a long distance (far-field), while requiring a small change in the existing wireless communication systems [4]–[6]. In addition, the energy sources of WPT systems is more stable than those of wind and solar systems [7], [8].

Along with advantages, there are also difficulties of WPT. The most challenging is the transmitted energy being

significantly deteriorated with the distance. To deal with this problem, beamforming techniques have been applied in WPT [9]–[13]. More precisely, papers [9]–[12] considered beamforming techniques for a multiple-input single-output systems, and [13] studied multiple-input multiple-output (MIMO) systems. Particularly, it was shown that by using optimal beamforming vectors, the power transfer efficiency is significantly improved [13].

Another aspect should be mentioned in WPT is the source of energy, which can be classified into two groups: i) dedicated RF sources and ii) ambient RF sources. While the first kind can be macro base stations or power beacons (PBs), the second one are neighbour RF sources (such as neighbor cellular users, base stations and access points), which are considered as passive energy sources. Literature shows that many previous works on WPT considered either dedicated sources [14]–[18] or ambient RF sources [19]–[23]. Recently, with an attempt to enhance the amount of harvested energy, Zhu *et al.* [24] exploited both kind of energies. To be more specific, [24] considered K -tier heterogeneous

networks (HetNets), in which a single-antenna user harvests energy from the dedicated source, i.e., the macro base station that the user associated with, and from ambient sources, i.e., the other network nodes such as neighbor macro base stations and neighbor small-cell base stations. The result illustrates the power transfer efficiency of the considered system is significantly improved.

Many previous works have considered the applications of WPT in many wireless systems such HetNets [25], [26], mmWave cellular networks [27], physical layer security [28], and non-orthogonal multiple access (NOMA) [29]. WPT has been also studied in the device to device (D2D) communication system, a promising technique in 5G, since D2D systems offer high spectral efficiency, low latency, and low transmit power [30]. Note that, in D2D communications, owing to the short distance between the transmitter and the receiver, the transmit power can be low, and hence, the application of SWP in D2D systems is very promising and has attracted a lot of research interest recently [31], [32]. Sakr and Hossain [31] analysed the performance of a D2D system in which the transmitter harvests energy from the ambient interference for spectrum random access and prioritized access. While in [32], the energy harvesting was considered in mobile user equipment relay systems. In this work, the user equipment relay collects energy from access points located at random following homogeneous Poison point process (HPPP).

Motivated by the above discussion, in this paper we propose and analyse a D2D system with WPT. Different from [31], we assume that the transmitter is equipped with multiple-energy-harvesting antennas, and harvests energy not only from the PB but also from the ambient RF sources. In addition, to enhance the power transfer efficiency from the PB to the transmitter, we apply a beamforming technique based on Rayleigh-Ritz theorem, which was introduced in [13], but here in our work the receiving power protocol is different. More precisely, the beamforming approach in [13] was considered under the power-splitting scheme. By contrast, in our work, we consider the time-splitting scheme. Note that, [12] showed that the time-splitting policy is simple to the implement and outperforms the power-splitting policy. The main contributions are summarized as follows:

- We propose a model in which the D2D transmitter harvests energy not only from the PB, but also from ambient RF sources whose distributions are modelled as HPPP. Particularly, to improve the power transfer efficiency, the D2D transmitter is proposed to equip with multiple antennas for harvesting the energy. Two beamforming approaches are proposed: optimal beamforming vector (OBV) and best antenna-based beamforming (BABB) at the power beacon.
- With the considered system, we derive exact analytical expressions of the average energy harvesting, power outage probability of the energy transfer phase, and outage probability of the information transmit phase. Our results show that, by using OBV beamforming technique and increasing the number of energy-harvesting

antennas at the D2D transmitter, the system performance can noticeably improves.

Notation: We use the following notation throughout this paper: bold upper-case, bold lower-case and non-bold letter are used to denote matrix, vector and scalar, respectively. $|\cdot|$, $\|\cdot\|$ and $[\cdot]^H$ denote the module, norm two and hermitian transpose. $\mathcal{L}(\cdot)$ and $\mathbb{E}\{\cdot\}$ present the Laplace transform function and expectation operator. \Im and $\Gamma(\alpha, \beta)$ are the imaginary function and Gamma function.

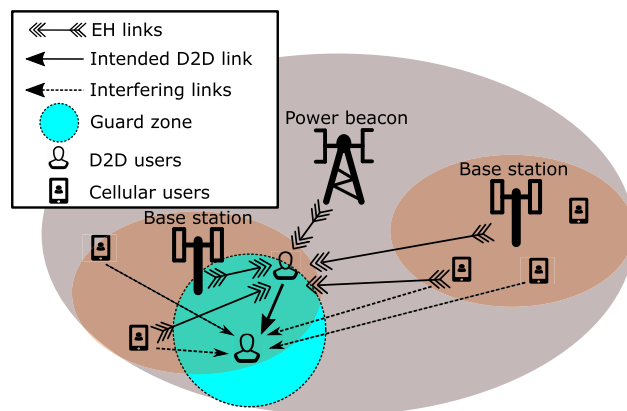


FIGURE 1. System model - in which base stations and neighbour cellular users play a role as the ambient RF sources.

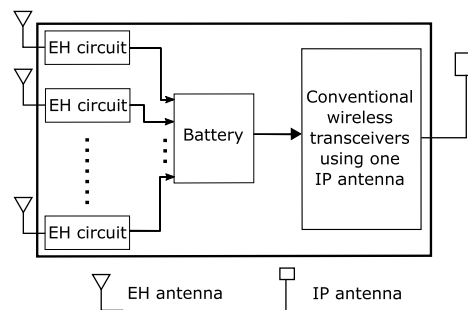


FIGURE 2. Receiver architecture designs for RF-powered information receiver - with multiple energy harvesting (EH) antennas and single information transceiver (IP) antenna.

II. NETWORK MODEL

We consider a wireless-powered D2D communication system as shown in Figure 1 which consists of a power beacon (PB) equipped with N_p antennas, a D2D transmitter T_x (equipped with N_E antennas for receiving energy and one antenna for informative purpose, see Figure 2),¹ a D2D single-antenna receiver R_x , a set of ambient RF sources, denoted by Φ_{RF} (e.g., the set of base stations), that operates with different frequency from the D2D link does, and a set of cellular users, denoted by Φ_I , that uses the same frequency

¹The D2D transmitter has a single antenna for information transmission due to its cost and physical size limitations. By contrast, it can deploy multiple antennas for harvesting energy since the RF energy harvesting circuit is small and simple [8], [33], [34].

and time resource as D2D link does. As a result, Φ_I interferes on the transmission between T_x and R_x . We assume that Φ_{RF} and Φ_I are modelled as homogeneous Poisson point process (HPPP) with density λ_{RF} and λ_I , respectively. Furthermore, we assume no interferer is closer R_x than z_0 m.

Let T be the time period for transmitting an information block from T_x to R_x . By applying time-splitting protocol, each block time T is divided into two phases as follows [7]:

1) PHASE 1–ENERGY HARVESTING PHASE

This phase is used for transfer energy from PB to T_x with the duration of τT , where $\tau \in (0, 1)$ is a time-splitting ratio.

To transfer energy to T_x , PB sends a signal $w s_p$, where $w \in \mathbb{C}^{N_p \times 1}$, $\mathbb{E}\{\|w\|^2\} = 1$, is the beamforming vector and s_p , $\mathbb{E}\{|s_p|^2\} = 1$, is the power symbol. In addition to the power received from PB, T_x also harvests energy from Φ_{RF} and Φ_I . Let $\bar{H} \in \mathbb{C}^{N_p \times N_E}$, $\bar{f}_r \in \mathbb{C}^{N_E \times 1}$ and $\bar{f}_i \in \mathbb{C}^{N_E \times 1}$ be the channel coefficient of the links from T_x to PB, to r -th RF source and to i -th interference, respectively. Note that the channels \bar{H} and \bar{f}_r include the small-scale fading and path loss expressed as a short-range propagation model as follows [35]:

$$\bar{H}^H = \sqrt{\mathcal{K} \max\left(\frac{d_{pt}}{d_0}, d_0\right)^{-\beta}} H^H, \quad (1)$$

and

$$\bar{f}_r = \sqrt{\mathcal{K} \max\left(\frac{d_i}{d_0}, d_0\right)^{-\alpha}} f_r, \quad (2)$$

where \mathcal{K} is a constant depending on the frequency, d_0 is the reference distance; α and β are the path-loss exponent; d_{pt} and d_i are the distances from T_x to PB and the i -th interference source, respectively. In addition, H and f_r represent the small-scale fading whose entries are independent and identically distributed (i.i.d.) zero-mean complex Gaussian random variables with unit variance. Then the total harvested energy at T_x at the end of the first phase is given by

$$E_k = \underbrace{\eta\tau TP_p \|\bar{H}^H w\|^2}_{E_{k,1}} + \underbrace{\sum_{r \in \Phi_{RF}} \eta\tau TP_{RF} \|\bar{f}_r\|^2}_{E_{k,2}} + \underbrace{\sum_{i \in \Phi_I} \eta\tau TP_I \|\bar{f}_i\|^2}_{E_{k,3}}, \quad (3)$$

where $k \in \{b, o\}$ denotes for beamforming scheme (which are described in detail in follow); η is the RF-DC transfer efficiency; P_p , P_{RF} and P_I are the transmit power of PB, ambient RF source and interference, respectively; $E_{k,1}$, $E_{k,2}$, $E_{k,3}$ represent for the harvested energy from PB, ambient RF source and interference, respectively. Due to low density of interferences and large distance between themselves to T_x , $E_{k,3}$ can be neglected.

In order to enhance the power transfer efficiency, we applied two beamforming schemes into the power transfer process, which are described as follows:

- Best Antenna Based-Beamforming (BABB): with BABB scheme, only one antenna at PB is used for power transfer. This antenna is chosen so that receive energy at T_x is maximal. Mathematically, the chosen antenna i^* is given by

$$i^* = \arg \max_{i=1, \dots, N_p} \left(\sum_{j=1}^{N_E} |h_{i,j}|^2 \right),$$

where $h_{i,j} \sim \mathcal{CN}(0, 1)$ is the (i, j) -th element of H . With BABB scheme, the beamforming vector w becomes the i^* -th column of I_{N_p} . Then, the total harvested energy (3) can be re-written as

$$E_b = \underbrace{\eta\tau T \mathcal{K} P_p \max\left(\frac{d_{pt}}{d_0}, d_0\right)^{-\beta} \sum_{j=1}^{N_E} |h_{i^*,j}|^2}_{E_{b,1}} + \underbrace{\eta\tau T \mathcal{K} P_{RF} \sum_{i \in \Phi_{RF}} |f_r|^2 \max\left(\frac{d_i}{d_0}, d_0\right)^{-\alpha}}_{E_{b,2}} \quad (4)$$

where $E_{b,1}$ and $E_{b,2}$ are the energies that T_x receives from PB and ambient RF sources, respectively.

- Optimal Beamforming Vector (OBV): with OBV scheme, PB uses all antennas for power transfer, and finds w to maximize the receive energy at T_x . More precisely, the optimal w^* is given by

$$w^* = \arg \max_{w \in \mathbb{C}^{N_p \times 1}} \|\bar{H}^H w\|^2. \quad (5)$$

From (1), we can re-write (5) as

$$w^* = \arg \max_{w \in \mathbb{C}^{N_p \times 1}} \|H^H w\|^2 = \arg \max_{w \in \mathbb{C}^{N_p \times 1}} w^H H H^H w. \quad (6)$$

Since $\|w\|^2 = 1$, $w^H H H^H w$ is a Rayleigh-Ritz quotient. Thus, from Rayleigh-Ritz Theorem [36], w^* is the unit-norm eigenvector corresponding to the largest eigenvalue of the Wishart matrix $H H^H$. Consequently, the total harvested energy (3) at T_x is re-expressed as

$$E_o = \underbrace{\eta\tau T \mathcal{K} P_p \max\left(\frac{d_{pt}}{d_0}, d_0\right)^{-\beta} \lambda_{max}}_{E_{o,1}} + \underbrace{\eta\tau T \mathcal{K} P_{RF} \sum_{i \in \Phi_{RF}} |f_r|^2 \max\left(\frac{d_i}{d_0}, d_0\right)^{-\alpha}}_{E_{o,2}}, \quad (7)$$

where λ_{max} is the largest eigenvalue of $H H^H$.

2) PHASE 2–DATA TRANSMISSION PHASE

The remaining duration, $(1 - \tau)T$, is used for the data transmission. More precisely, the source uses energy harvested in the energy harvesting phase to transmit signal to the destination.

Let s and s_i , where $E\{|s|^2\} = E\{|s_i|^2\} = 1$, be the signals transmitted from T_x and the i -th interference source, respectively. The received signal at DU_{R_x} , then, can be expressed as

$$y_{r,k} = \sqrt{\frac{E_k}{(1-\tau)T}} \bar{h}_{tr}s + \sum_{i \in \Phi_1} \sqrt{P_1 \bar{g}_i} s_i + n_r, \quad (8)$$

where $k \in \{b, o\}$ depends the beamforming schemes at PB, \bar{h}_{tr} and \bar{g}_i are the channel coefficients of $T_x - R_x$ link and the i -th interference source - R_x link, and n_r is the AWGN with zero-mean and variance N_0 .

The channel \bar{h}_{tr} and \bar{g}_i are modelled as follows:

$$\bar{h}_{tr} = \sqrt{\mathcal{K} \max\left(\frac{d_{tr}}{d_0}, 1\right)^{-\alpha}} h_{tr}, \quad (9)$$

and

$$\bar{g}_i = \sqrt{\mathcal{K} d_{ir}^{-\alpha}} g_i, \quad (10)$$

where d_{tr} and d_{ir} are the distances from R_x to T_x and i -th interference source, respectively. In addition, $h_{tr} \sim \mathcal{CN}(0, 1)$ and $g_i \sim \mathcal{CN}(0, 1)$ represent the small-scale fading.

Finally, the end-to-end signal to interference plus noise ratio (SINR) is given by

$$\gamma_k = \frac{\frac{E_k}{(1-\tau)T} |\bar{h}_{tr}|^2}{N_0 + \sum_{i \in \Phi_1} P_1 |\bar{g}_i|^2}. \quad (11)$$

III. ENERGY AND OUTAGE PROBABILITY ANALYSIS

In this section, we evaluate the efficiency of wireless power transfer in terms of average harvesting energy, power outage probability, and the outage probability of the D2D link. These metrics are defined and analysed in details in the following subsections.

A. LAPLACE TRANSFORM FUNCTION

We provide some basic results which can be used for the derivations of energy analysis and outage probability in Sections III-B, III-C and III-D.

Let Φ be set of points following HPPP with density λ , and d_i is the distance between the i -th point in Φ and the origin. We define random variables \mathcal{Z}_1 and \mathcal{Z}_2 as

$$\mathcal{Z}_1 \triangleq \sum_{i \in \Phi} X_i \mathcal{K} \max(d_i, l_0)^{-\alpha}, \quad (12)$$

and

$$\mathcal{Z}_2 \triangleq \sum_{i \in \Phi} X_i \mathcal{K} d_i^{-\alpha} \mathbb{1}(d_i > z_0), \quad (13)$$

where l_0, \mathcal{K} , are positive constants, $\alpha \geq 2$, $\{X_i\}, i \in \Phi$, are i.i.d. Gamma distributed with shape N and phase 1, i.e., $X_i \sim \Gamma(N, 1)$. Then we have the following result.

Lemma 1: The Laplace transform function of random variable \mathcal{Z}_1 given by (12) is calculated by

$$\begin{aligned} \mathcal{L}_{\mathcal{Z}_1}(s) &= \exp \left\{ \pi \lambda \left[-\mathcal{K}_0^{2/\alpha} s^{2/\alpha} \frac{\Gamma(N+2/\alpha) \Gamma(1-2/\alpha)}{\Gamma(N)} \right. \right. \\ &\quad \left. \left. + \frac{\mathcal{K}_0 N s l_0^{2-\alpha}}{(N+2/\alpha)(\mathcal{K}_0 l_0^{-\alpha} s + 1)^{N+1}} \right] \right\} \\ &\quad \times {}_2F_1 \left(1, N+1; N+1 + \frac{2}{\alpha}; \frac{1}{\mathcal{K}_0 l_0^{-\alpha} s + 1} \right) \end{aligned} \quad (14)$$

where $\Gamma(\cdot)$ is the Gamma function, and ${}_2F_1(\cdot, \cdot; \cdot; \cdot)$ is the hyper-geometric function [37].

Proof: See Appendix A. ■

Lemma 2: With random variable \mathcal{Z}_2 being defined as in (13), its Laplace transform function is expressed as follows:

$$\begin{aligned} \mathcal{L}_{\mathcal{Z}_2}(s) &= \exp \left\{ \pi \lambda \left[z_0^2 \left(1 - \frac{1}{(1+s\mathcal{K}z_0^{-\alpha})^N} \right) \right. \right. \\ &\quad \left. \left. - \mathcal{K}^{2/\alpha} s^{2/\alpha} \frac{\Gamma(N+2/\alpha) \Gamma(1-2/\alpha)}{\Gamma(N)} \right] \right\} \\ &\quad + \frac{sN\mathcal{K}z_0^{2-\alpha}}{(N+2/\alpha)(s\mathcal{K}z_0^{-\alpha} + 1)^{N+1}} \\ &\quad \times {}_2F_1 \left(1, N+1; N+1 + \frac{2}{\alpha}; \frac{1}{s\mathcal{K}z_0^{-\alpha} + 1} \right) \end{aligned} \quad (15)$$

Proof: Following a similar methodology used in the derivations of $\mathcal{L}_{\mathcal{Z}_1}(s)$ in Lemma 1. ■

Lemma 3: The Laplace transform function of

$$\mathcal{Z}_3 \triangleq \max_{i=1, \dots, N} \left\{ \sum_{j=1}^M |h_{i,j}|^2 \right\},$$

where $h_{i,j} \sim \mathcal{CN}(0, 1)$, N and M are positive integers, is given by

$$\begin{aligned} \mathcal{L}_{\mathcal{Z}_3}(s) &= \sum_{m=0}^N \sum_{(k_0 + \dots + k_{M-1} = m)} C(M, m, \mathbf{k}) A(M, m, \mathbf{k})! \\ &\quad \times \frac{s}{(s+m)^{A(M, m, \mathbf{k})+1}}, \end{aligned} \quad (16)$$

where $\mathbf{k} \triangleq \{k_0, \dots, k_{M-1}\}$,

$$C(M, m, \mathbf{k}) \triangleq (-1)^m \binom{N}{m} \binom{m}{k_0, \dots, k_{M-1}} \prod_{q=0}^{M-1} \frac{1}{(q!)^{k_q}}, \quad (17)$$

$$A(M, m, \mathbf{k}) \triangleq \sum_{t=0}^{M-1} t k_t. \quad (18)$$

Proof: See Appendix B. ■

B. AVERAGE HARVESTED ENERGY

The instantaneous harvested energy changes over time due to the random nature of propagation. Thus, to evaluate the amount of harvested energy, we derive the expressions for average harvested energy for two beamforming schemes as follows.

Theorem 1: The average harvested energy in phase 1 for BABB scheme is given by

$$\bar{E}_b = \eta\tau T\mathcal{K}_0 \left\{ \pi\lambda_{\text{RF}}N_{\text{E}}P_{\text{RF}} \left(\frac{\alpha}{\alpha-2} \right) - P_{\text{p}} \max \left(\frac{d_{\text{pt}}}{d_0}, d_0 \right)^{-\beta} \times \sum_{m=1}^{N_{\text{p}}} \sum_{(k_0+\dots+k_{N_{\text{E}}-1}=m)} C(N_{\text{E}}, m, \mathbf{k}) \frac{A(N_{\text{E}}, m, \mathbf{k})!}{m^{A(N_{\text{E}}, m, \mathbf{k})+1}} \right\}. \quad (19)$$

Proof: See Appendix C ■

Remark 1: The term $\eta\tau T\mathcal{K}_0 \left(\pi\lambda_{\text{RF}}N_{\text{E}}P_{\text{RF}} \frac{\alpha}{\alpha-2} \right)$ in (19) shows that the average harvested energy from ambient radio frequency sources increases linearly with N_{E} . Therefore, by deploying multiple antenna at T_x , we take the benefit of harvesting energy ambient radio frequency sources.

Theorem 2: Let define $N_{\lambda} \triangleq \min(N_{\text{p}}, N_{\text{E}})$, then the average energy that T_x harvests from PB and ambient radio frequency sources for OBV scheme is given by

$$\bar{E}_o = \eta\tau T\mathcal{K}_0 P_{\text{p}} \max \left(\frac{d_{\text{pt}}}{d_0}, d_0 \right)^{-\beta} \sum_{i=1}^{N_{\lambda}} \sum_{m=|N_{\text{p}}-N_{\text{E}}|}^{(N_{\text{p}}+N_{\text{E}})i-2i^2} (m+1) \times \frac{d_{i,m}}{i} + \eta\tau T\pi\mathcal{K}_0\lambda_{\text{RF}}N_{\text{E}}P_{\text{RF}} \left(1 + \frac{2}{\alpha-2} \right), \quad (20)$$

where

$$d_{i,m} \triangleq \frac{m!c_{i,m}}{i^{m+1} \left[\prod_{i=1}^{N_{\lambda}} (N_{\text{E}} - i)!(N_{\text{p}} - i)! \right]},$$

and $c_{i,m}$ are constants computed as in [38].

Proof: From (7), the instantaneous received energy from the PB is

$$E_{o,1} = \eta\tau T\mathcal{K}_0 P_{\text{p}} \max \left(\frac{d_{\text{pt}}}{d_0}, d_0 \right)^{-\beta} \lambda_{\text{max}}. \quad (21)$$

Recall that λ_{max} is the largest eigenvalue of HH^H . The PDF of λ_{max} is given by [38]

$$f_{\lambda_{\text{max}}}(x) = \sum_{i=1}^{N_{\lambda}} \sum_{m=|N_{\text{p}}-N_{\text{E}}|}^{(N_{\text{p}}+N_{\text{E}})i-2i^2} \frac{d_{i,m} i^{m+1} x^m \exp(-ix)}{m!}, \quad (22)$$

Using (22), after some manipulations, the Laplace transform function of λ_{max} is

$$\mathcal{L}_{\lambda_{\text{max}}}(s) = \sum_{i=1}^{N_{\lambda}} \sum_{m=|N_{\text{p}}-N_{\text{E}}|}^{(N_{\text{p}}+N_{\text{E}})i-2i^2} d_{i,m} \frac{i^{m+1}}{(i+s)^{m+1}}. \quad (23)$$

As a result, the average harvested energy $\bar{E}_{o,1}$ can be found by taking the derivative of $\mathcal{L}_{\lambda_{\text{max}}}(s)$ with respect to s and set $s = 0$.

Note that the instantaneous harvested energy $E_{o,2}$ from the ambient RF sources is equal to $E_{b,2}$ in (4). Thus, the derivation of $\bar{E}_{o,2}$ has been already proved in Appendix C. ■

C. POWER OUTAGE PROBABILITY

In reality, the amount of energy that T_x harvests from the first phase has to exceed a certain value defined as a threshold P_{th} . Thus, in this part we analyze the power outage probability which is defined as the probability that the harvested power is less than P_{th} . Mathematically, the power outage probability is given by

$$H_k = \Pr \left\{ \frac{E_k}{(1-\tau)T} < P_{\text{th}} \right\}, \quad (24)$$

where $\frac{E_k}{(1-\tau)T}$ is harvested power, $k = \{b,o\}$ corresponds to BAS and OBV schemes, respectively.

Theorem 3: If the PB employs BABB policy, the power outage probability is then given by

$$H_b = \frac{1}{2} - \frac{1}{\pi} \int_0^{\infty} \frac{1}{w} \Im \left\{ \exp(-j\bar{P}_{\text{th}}w) \mathcal{L}_{\mathcal{X}_2}(-jP_{\text{RF}}w) \times \mathcal{L}_{\mathcal{X}_1} \left(-jP_{\text{p}}\mathcal{K}_0 \max \left(\frac{d_{\text{pt}}}{d_0}, d_0 \right)^{-\beta} w \right) \right\} dw, \quad (25)$$

where $\bar{P}_{\text{th}} = \frac{(1-\tau)P_{\text{th}}}{\eta\tau}$,

$$\mathcal{L}_{\mathcal{X}_1}(s) = \sum_{m=0}^{N_{\text{p}}} \sum_{(k_0+\dots+k_{N_{\text{E}}-1}=m)} C(N_{\text{E}}, m, \mathbf{k}) A(N_{\text{E}}, m, \mathbf{k})! \times \frac{s}{(s+m)^{A(N_{\text{E}}, m, \mathbf{k})+1}}, \quad (26)$$

and

$$\begin{aligned} \mathcal{L}_{\mathcal{X}_2}(s) &= \exp \left\{ \pi\lambda_{\text{RF}} \left[-\mathcal{K}_0^{2/\alpha} s^{2/\alpha} \frac{\Gamma(N_{\text{E}}+2/\alpha)\Gamma(1-2/\alpha)}{\Gamma(N_{\text{E}})} \right. \right. \\ &\quad \left. \left. + \frac{N\mathcal{K}_0 s}{(N_{\text{E}}+2/\alpha)(\mathcal{K}_0 s+1)^{N_{\text{E}}+1}} \right] \right. \\ &\quad \left. \times {}_2F_1 \left(1, N_{\text{E}}+1; N_{\text{E}}+1 + \frac{2}{\alpha}; \frac{1}{\mathcal{K}_0 s+1} \right) \right\}. \end{aligned} \quad (27)$$

Proof: Equation (4) can be re-written as

$$E_b = \eta\tau T \left(P_{\text{p}}\mathcal{K}_0 \max \left(\frac{d_{\text{pt}}}{d_0}, d_0 \right)^{-\beta} \mathcal{X}_1 + P_{\text{RF}}\mathcal{X}_2 \right), \quad (28)$$

where $\mathcal{X}_1 \triangleq \max_{i=1, \dots, N_{\text{p}}} \left(\sum_{j=1}^{N_{\text{E}}} |h_{i,j}|^2 \right)$, $\mathcal{X}_2 \triangleq \sum_{i \in \Phi_{\text{RF}}} |f_r|^2 \mathcal{K}_0 \max \left(\frac{d_i}{d_0}, d_0 \right)^{-\alpha}$. By substituting (28) into (24), we have

$$H_b = \Pr \left\{ \frac{\eta\tau W_b}{1-\tau} < P_{\text{th}} \right\} = F_{W_b}(\bar{P}_{\text{th}}), \quad (29)$$

where $W_b \triangleq P_p \mathcal{K}_0 \max\left(\frac{d_{pt}}{d_0}, d_0\right)^{-\beta} \mathcal{X}_1 + P_{RF} \mathcal{X}_2$. To find the CDF of W_b , we first use Lemma 1 and Lemma 3 to derive the Laplace transform function of $P_p \mathcal{K}_0 \max\left(\frac{d_{pt}}{d_0}, d_0\right)^{-\beta} \mathcal{X}_1 + P_{RF} \mathcal{X}_2$. Then, we apply the Gil-Palaez theorem [39] to obtain the final result. ■

Theorem 4: If the PB employs OBV policy, the power outage probability is given by

$$H_o = \frac{1}{2} - \frac{1}{\pi} \int_0^\infty \frac{1}{w} \Im \left\{ \exp(-j\bar{P}_{th}w) \mathcal{L}_{\mathcal{X}_2}(-jP_{RF}w) \times \mathcal{L}_{\mathcal{X}_3} \left(-jP_p \mathcal{K}_0 \max\left(\frac{d_{pt}}{d_0}, d_0\right)^{-\beta} w \right) \right\} dw, \quad (30)$$

where $\mathcal{L}_{\mathcal{X}_3}(s)$ is the Laplace transform function of λ_{max} as in (23).

Proof: Following a similar methodology used in the derivations of H_b in Theorem 3. ■

D. OUTAGE PROBABILITY

In this section, we analyze the system performance in terms of outage probability of the transmission from T_x to R_x (D2D link) for BABB and OBV schemes at the PB.

1) BEST ANTENNA BASED-BEAMFORMING

The system capacity for BABB scheme is given by

$$C_b = \log_2(1 + \gamma_b), \quad (31)$$

where γ_b is expressed as in (11).

For a given threshold R_{th} , the outage probability is defined as

$$P_b = \Pr\{C_b < R_{th}\}. \quad (32)$$

By using Lemma 2, we obtain the following analytical expression for the outage probability given by (32).

Theorem 5: For the BABB scheme, the outage probability of the D2D link is given by

$$P_b = \frac{1}{2} - \frac{1}{\pi} \int_{h=0}^\infty \int_{w=0}^\infty \frac{1}{w} \Im \left\{ \exp\left(-j\frac{\bar{\gamma}_{th}w}{x_3}\right) \times \mathcal{L}_{\mathcal{X}_1} \left(-jP_p \mathcal{K}_0 \max\left(\frac{d_{pt}}{d_0}, d_0\right)^{-\beta} w \right) \times \mathcal{L}_{\mathcal{X}_2}(-jP_{RF}w) \mathcal{L}_{\mathcal{X}_4} \left(\frac{P_1 \bar{\gamma}_{th} w}{x_3} \right) \right\} \exp(-x_3) dx_3 dw, \quad (33)$$

where $\bar{\gamma}_{th} \triangleq \frac{1-\tau}{\eta\tau\mathcal{K}_0} (2^{R_{th}} - 1) \max\left(\frac{d_{tr}}{d_0}, d_0\right)^\alpha$,

$$\begin{aligned} \mathcal{L}_{\mathcal{X}_4}(s) &= \exp \left\{ \pi \lambda_1 \left[z_0^2 \left(1 - \frac{1}{(1 + s \mathcal{K}_0 z_0^{-\alpha})^{N_E}} \right) - s^{2/\alpha} \mathcal{K}_0^{2/\alpha} \frac{\Gamma(N_E + 2/\alpha) \Gamma(1 - 2/\alpha)}{\Gamma(N_E)} \right] \right\} \end{aligned}$$

$$+ \frac{s N_E \mathcal{K}_0 z_0^{2-\alpha}}{(N_E + 2/\alpha) (s \mathcal{K}_0 z_0^{-\alpha} + 1)^{N_E+1}} \times {}_2F_1 \left(1, N_E + 1; N_E + 1 + \frac{2}{\alpha}; \frac{1}{s \mathcal{K}_0 z_0^{-\alpha} + 1} \right) \Bigg\}, \quad (34)$$

and where z_0 is radius of the guard zone.

Proof: By substituting (31) into (32) and using γ_b in (11) for $k = b$, we have

$$\begin{aligned} P_b &= \Pr \left\{ W_b < \bar{\gamma}_{th} \frac{N_0 + P_1 \mathcal{X}_4}{\mathcal{X}_3} \right\} \quad (35) \\ &= \int_0^\infty \int_0^\infty F_{W_b} \left(\bar{\gamma}_{th} \frac{N_0 + P_1 x_4}{x_3} \right) f_{\mathcal{X}_3}(x_3) f_{\mathcal{X}_4}(x_4) dx_4 dx_3 \\ &\stackrel{(c)}{=} \int_0^\infty \int_0^\infty \left[\frac{1}{2} - \frac{1}{\pi} \int_{w=0}^\infty \frac{1}{w} \Im \left\{ \exp\left(-j\bar{\gamma}_{th} \frac{N_0 + P_1 x_4}{x_3} w\right) \times \mathcal{L}_{\mathcal{X}_1}(-jP_p \mathcal{K}_0 \max\left(\frac{d_{pt}}{d_0}, d_0\right)^{-\beta} w) \mathcal{L}_{\mathcal{X}_2}(-jP_{RF}w) \right\} dw \right] \\ &\quad \times f_{\mathcal{X}_3}(x_3) f_{\mathcal{X}_4}(x_4) dx_4 dx_3 \quad (36) \\ &\stackrel{(d)}{=} \frac{1}{2} - \frac{1}{\pi} \int_0^\infty \int_{w=0}^\infty \frac{1}{w} \Im \left\{ \exp\left(-j\frac{N_0 \bar{\gamma}_{th} w}{x_3}\right) \times \mathcal{L}_{\mathcal{X}_1}(-jP_p \mathcal{K}_0 \max\left(\frac{d_{pt}}{d_0}, d_0\right)^{-\beta} w) \times \mathcal{L}_{\mathcal{X}_2}(-jP_{RF}w) \mathcal{L}_{\mathcal{X}_4} \left(\frac{P_1 \bar{\gamma}_{th} w}{x_3} \right) \exp(-x_3) \right\} dx_3 dw, \quad (37) \end{aligned}$$

where (c) is hold by using Gil-Palaez theorem, (d) is achieved by using the definition of Laplace transform function of variable \mathcal{X}_4 , $\mathcal{X}_3 \triangleq |h_{tr}|^2$, $\mathcal{X}_4 \triangleq \sum_{i \in \Phi_1} \mathcal{K}_0 d_{ir}^{-\alpha} g_i \mathbb{1}(d_{ir} > z_0)$, $f_{\mathcal{X}_3} = \exp(-x_3)$ and $f_{\mathcal{X}_4}(x_4)$ are the PDF of variables \mathcal{X}_3 and \mathcal{X}_4 , respectively. ■

2) OPTIMAL BEAMFORMING VECTORS SCHEME

Theorem 6: The expression of the outage probability for OBV scheme is given by

$$P_o = \frac{1}{2} - \frac{1}{\pi} \int_{h=0}^\infty \int_{w=0}^\infty \frac{1}{w} \Im \left\{ \exp\left(-j\frac{\bar{\gamma}_{th} N_0 w}{x_3}\right) \times \mathcal{L}_{\mathcal{X}_1} \left(-jP_p \mathcal{K}_0 \max\left(\frac{d_{pt}}{d_0}, d_0\right)^{-\beta} w \right) \times \mathcal{L}_{\mathcal{X}_2}(-jP_{RF}w) \mathcal{L}_{\mathcal{X}_4} \left(\frac{P_1 \bar{\gamma}_{th} w}{x_3} \right) \right\} \exp(-x_3) dx_3 dw, \quad (38)$$

where $\bar{\gamma}_{th}$ and the Laplace transform function $\mathcal{L}_{\mathcal{X}_4}(s)$ are defined as in Theorem 5, $\mathcal{L}_{\mathcal{X}_1}(s)$, $\mathcal{L}_{\mathcal{X}_2}(s)$ and $\mathcal{L}_{\mathcal{X}_3}(s)$ are defined in (26), (27) and (23), respectively.

Proof: Following a similar methodology used in the derivations of P_o in Theorem 5. ■

IV. NUMERICAL RESULTS

In this section, simulation results based on Monte Carlo method are provided to verify the accuracy of our analytical results. Furthermore, the system performance is analysed and investigated for different network parameters.

A. NETWORK PARAMETERS

For simulations, network parameters are chosen as follows:

- The operating frequency for power and information phases is assumed at $f_c = 1$ GHz, with the bandwidth $BW = 10$ MHz.
- Time-splitting ratio is $\tau = 0.5$ and T is normalized to 1.
- The RF-DC transform efficiency of energy harvesting circuit is $\eta = 0.8$.
- The path loss exponent of the PB- T_x link is $\beta = 2$ (for a short range), and the path loss exponent of the remainder links is $\alpha = 3$.
- The distances between the PB and T_x (d_{pt}), T_x and R_x (d_{tr}) are 10 meters.
- The noise figure is $N_f = 10$ dB, the noise power is $\sigma_2 = -170 + 10 \log_{10} BW + N_f = -90$ dBm.
- $K_0 = \left(\frac{C}{4\pi f_c}\right)^2 = 5.7 \times 10^{-4}$, where the reference distance d_0 is set to 1 and $C = 3 \times 10^8$ [24].

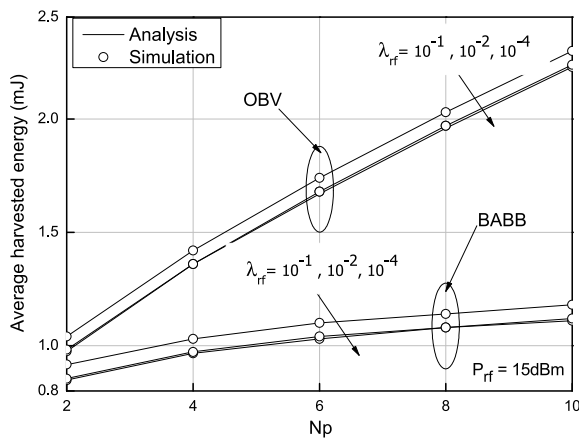


FIGURE 3. Average harvested energy with the various λ_{RF} .

B. AVERAGE HARVESTED ENERGY

Figure 3 shows the average harvested energy in mJ versus the number of PB antennas. We can see that the average harvested energy increases as the number of PB antennas. This implies that the average harvested energy can be improved by deploying more antennas at the PB. In addition, when the ambient RF sources density increases the performance also improves. The figure also shows that the OBV scheme outperforms the BABB scheme.

Next, we investigate the impact of the transmit power of the ambient RF sources on the average harvested energy,

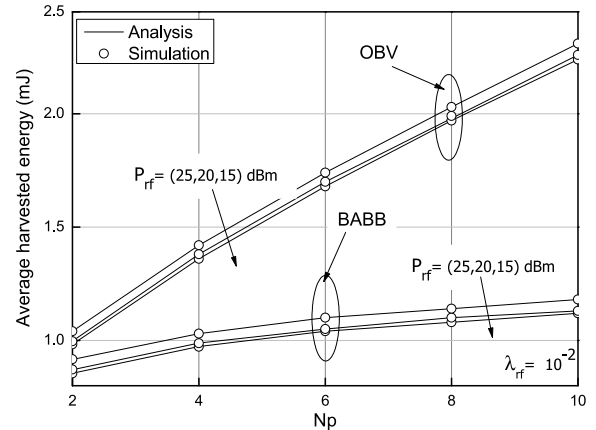


FIGURE 4. Average harvested energy with the various P_{rf} .

see Figure 4. Figure 4 illustrates that if the transmit power of ambient RF sources increases, the average harvested energy is improved. In addition, this improvement can increase with increment in the number of PB antennas.

In Figures 5 and 6, the average harvested energy is generated at large N_p . The results show that the amount of average harvested energy for OBV grows up to 11 mJ at $N_p = 100$. Note that in [24, Fig. 4], to reach this energy value, the number of transmit antennas is around 1000. To obtain the same average harvested energy level, the number of PB antennas can be significantly reduced by deploying multiple antennas for receiving energy at T_x .

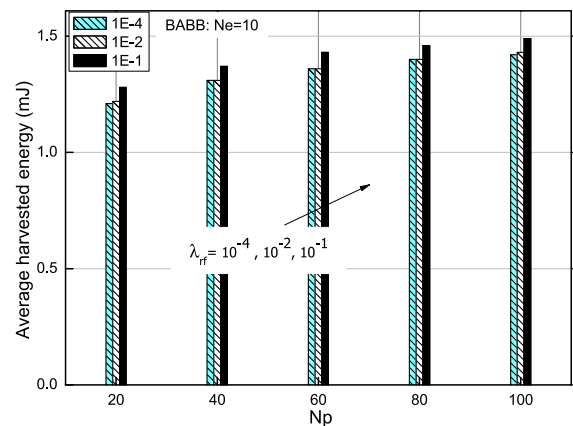


FIGURE 5. BABB: Average harvested energy with high N_p .

C. POWER OUTAGE PROBABILITY

In terms of power outage probability, Figure 7 shows that for OBV scheme, the power outage probability significantly reduces when the number of PB antennas increases. In the other words, power outage probability for BABB scheme slowly enhances with the increase in N_p .

Similarly, Figure 7 and 8 show the effects of the transmit power of ambient RF sources on the power outage probability. The increase of P_{RF} leads to the increase of the harvested energy, resulting in better performance.

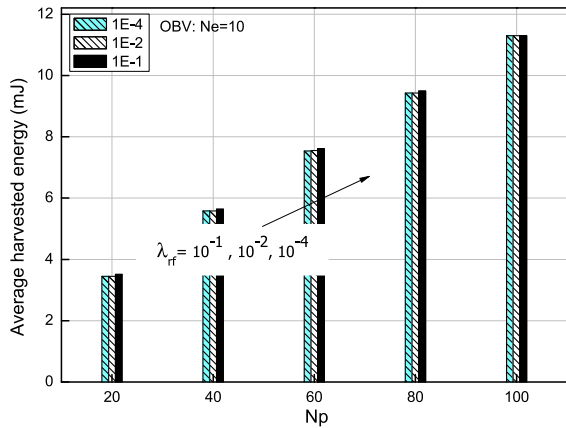


FIGURE 6. OBV: Average harvested energy with high N_p .

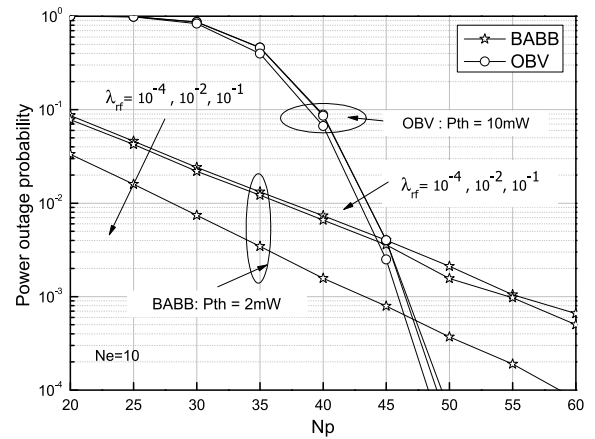


FIGURE 9. Power outage probability with high N_p .

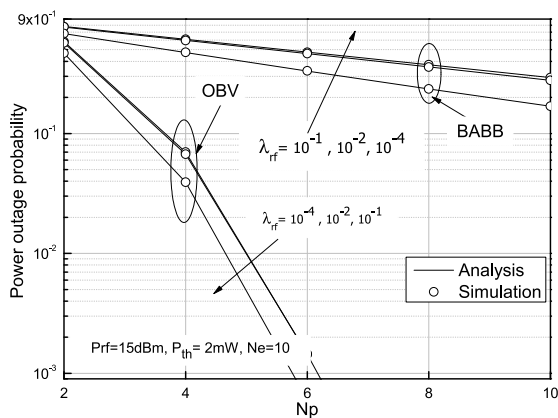


FIGURE 7. Power outage probability with various λ_{RF} .

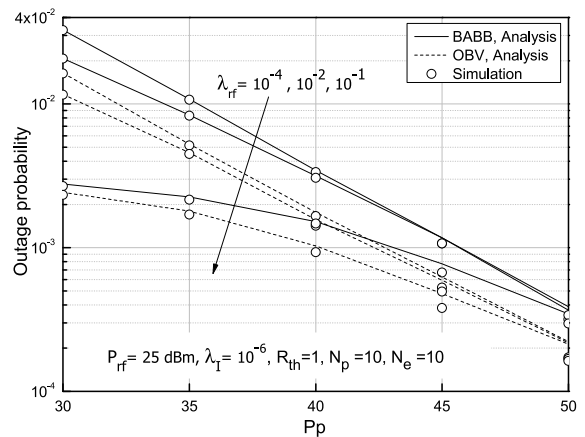


FIGURE 10. Outage probability.

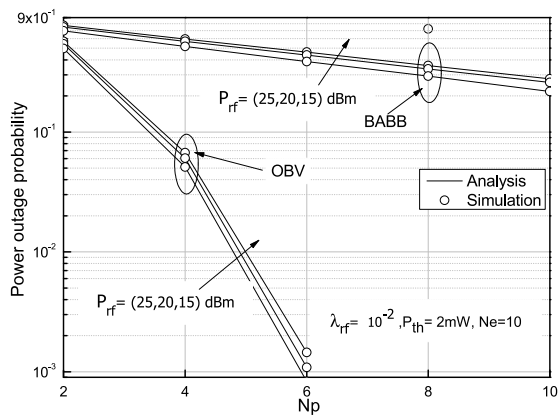


FIGURE 8. Power outage probability with various P_{rf} .

Particularly, Figure 9 shows that with $P_{th} = 10mW$, when $N_p > 45$, the power outage probability of the OBV scheme is significantly better than that of the BABB scheme.

D. OUTAGE PROBABILITY

Figure 10 shows that the outage probability decreases with the increment in P_p . In particular, the impact of ambient RF sources is more significant at small P_p . This comes from the fact that at high P_p , the energy that harvested from P_p become dominated.

V. CONCLUSIONS

This work proposed and analysed the performance of the energy harvesting-based D2D networks in the presence of interference and ambient RF sources. The D2D transmitter harvests energy from power beacon and the ambient RF sources. Two beamforming schemes are proposed at the PB to increase the power transfer efficiency. By applying the stochastic geometry tool, the exact analytical expressions for the OP and the average harvested energy were derived. We showed that the system performance can be significantly improved by deploying multiple antennas for energy harvesting at the D2D transmitter together with the use of OBV scheme at the PB.

APPENDIX A PROOF OF LEMMA 1

The Laplace transform of \mathcal{Z}_1 is given by

$$\begin{aligned} \mathcal{L}_{\mathcal{Z}_1}(s) &= \mathbb{E}[\exp(-s\mathcal{Z}_1)] \\ &= \mathbb{E}\left[\exp\left(-s \sum_{i \in \Phi} X_i \mathcal{K} \max(d_i, l_0)^{-\alpha}\right)\right]. \end{aligned}$$

$$\begin{aligned}
 &= \exp \left\{ -\lambda \mathbb{E}_{\mathcal{X}} \left[\int_0^{\infty} [1 - \exp(-sX\mathcal{K} \max(r, l_0)^{-\alpha})] \right. \right. \\
 &\quad \left. \left. \times 2\pi r dr \right] \right\} \\
 &= \underbrace{\exp \left\{ -\lambda \mathbb{E}_{\mathcal{X}} \left[\int_0^{l_0} [1 - \exp(-sX\mathcal{K}l_0^{-\alpha})] 2\pi r dr \right] \right\}}_{\mathcal{L}_1(s)} \\
 &\quad \times \underbrace{\exp \left\{ -\lambda \mathbb{E}_{\mathcal{X}} \left[\int_{l_0}^{\infty} [1 - \exp(-sX\mathcal{K}r^{-\alpha})] 2\pi r dr \right] \right\}}_{\mathcal{L}_2(s)}
 \end{aligned} \tag{A.1}$$

The term $\mathcal{L}_1(s)$ can be obtained by first taking integral with respect to variable r , then compute the expectation over \mathcal{X} as

$$\mathcal{L}_1(s) = \exp \left\{ -\pi \lambda l_0^2 \left(1 - \frac{1}{(1 + \mathcal{K}l_0^{-\alpha}s)^N} \right) \right\}. \tag{A.2}$$

The term $\mathcal{L}_2(s)$ can be derived as follows:

$$\begin{aligned}
 \mathcal{L}_2(s) &\stackrel{(a)}{=} \exp \left\{ \pi \lambda \left[l_0^2 \mathbb{E}_{\mathcal{X}} \left(1 - \exp(-s\mathcal{X}\mathcal{K}l_0^{-\alpha}) \right) \right. \right. \\
 &\quad - \mathcal{K}^{2/\alpha} s^{2/\alpha} \mathbb{E}_{\mathcal{X}} \left(\mathcal{X}^{2/\alpha} \right) \Gamma(1 - 2/\alpha) \\
 &\quad \left. \left. + \mathcal{K}^{2/\alpha} s^{2/\alpha} \mathbb{E}_{\mathcal{X}} \left(\mathcal{X}^{2/\alpha} \Gamma(1 - 2/\alpha, s\mathcal{K}\mathcal{X}l_0^{-\alpha}) \right) \right] \right\} \\
 &\stackrel{(b)}{=} \exp \left\{ \pi \lambda \left[l_0^2 \left(1 - \frac{1}{(1 + \mathcal{K}sl_0^{-\alpha})^N} \right) \right. \right. \\
 &\quad - \mathcal{K}^{2/\alpha} s^{2/\alpha} \frac{\Gamma(N + 2/\alpha) \Gamma(1 - 2/\alpha)}{\Gamma(N)} \\
 &\quad + \frac{\mathcal{K}Nl_0^{2-\alpha}s}{(N + 2/\alpha)(\mathcal{K}l_0^{-\alpha}s + 1)^{N+1}} \\
 &\quad \left. \left. \times {}_2F_1 \left(1, N + 1; N + 1 + \frac{2}{\alpha}; \frac{1}{\mathcal{K}l_0^{-\alpha}s + 1} \right) \right] \right\},
 \end{aligned} \tag{A.3}$$

where (a) follows the method of integration by parts as in [35], and (b) is obtained by taking the expectation over \mathcal{X} with the help of [37, 6.455]. By substituting $\mathcal{L}_1(s)$ and $\mathcal{L}_2(s)$ into (A.1), we arrive at the final result.

**APPENDIX B
PROOF OF LEMMA 3**

The CDF of $\mathcal{Z}_3 = \max_{j=1, \dots, N} \left\{ \sum_{j=1}^M |h_{i,j}|^2 \right\}$ is

$$\begin{aligned}
 F_{\mathcal{Z}_3}(x) &= \left(1 - \sum_{n=0}^{M-1} \frac{x^n}{n!} \exp(-x) \right)^N \\
 &= \sum_{m=0}^N (-1)^m \binom{N}{m} \left(\sum_{n=0}^{M-1} \frac{x^n}{n!} \exp(-x) \right)^m \\
 &= \sum_{m=0}^N \sum_{k_0 + \dots + k_{M-1} = m} C(M, m, \mathbf{k}) x^{A(M, m, \mathbf{k})} \exp(-mx),
 \end{aligned} \tag{B.1}$$

Then, the PDF of \mathcal{Z}_3 is obtained by taking the derivative of $F_{\mathcal{Z}_3}(x)$ with respect to x as follows:

$$\begin{aligned}
 f_{\mathcal{Z}_3}(x) &= \sum_{m=0}^N \sum_{(k_0 + \dots + k_{M-1} = m)} C(M, m, \mathbf{k}) \\
 &\quad \times \left[A(M, m, \mathbf{k}) x^{A(M, m, \mathbf{k})-1} - m x^{A(M, m, \mathbf{k})} \right] \exp(-mx).
 \end{aligned} \tag{B.2}$$

Finally, from (B.2), we get the Laplace transform function of \mathcal{Z}_3 .

**APPENDIX C
PROOF OF THEOREM 1**

The first and the second terms of (4) represent the harvested energy from the power beacon and the ambient RF sources, respectively. By applying the lemma 1 and lemma 3, we obtain the Laplace transform of two that terms. Then, taking the first derivative of these Laplace transform functions at $s = 0$, we obtain the average harvested energy as follows:

A. ENERGY FROM THE POWER BEACON

by applying Lemma 3, the Laplace transform of $E_{b,1}$ is

$$\begin{aligned}
 \mathcal{L}_{E_{b,1}}(s) &= \eta \tau T \mathcal{K}_0 P_p \max \left(\frac{d_{pt}}{d_0}, d_0 \right)^{-\beta} \\
 &\quad \times \sum_{m=0}^{N_p} \sum_{(k_0 + \dots + k_{N_E-1} = m)} \frac{s A(N_E, m, \mathbf{k})! C(N_E, m, \mathbf{k})}{(s + m)^{A(N_E, m, \mathbf{k})+1}}.
 \end{aligned} \tag{C.1}$$

Therefore, the average harvested energy from the power beacon is given by

$$\begin{aligned}
 \bar{E}_{b,1} &= - \frac{d \mathcal{L}_{E_{b,1}}(s)}{ds} \Big|_{s=0} \\
 &= - \eta \tau T \mathcal{K}_0 P_p \max \left(\frac{d_{pt}}{d_0}, d_0 \right)^{-\beta} \\
 &\quad \times \sum_{m=0}^{N_p} \sum_{(k_0 + \dots + k_{N_E-1} = m)} C(N_E, m, \mathbf{k}) \frac{A(N_E, m, \mathbf{k})!}{m^{A(N_E, m, \mathbf{k})+1}}.
 \end{aligned} \tag{C.2}$$

B. ENERGY FROM THE AMBIENT RF SOURCES

The average harvested energy from ambient RF source is computed by

$$\begin{aligned}
 \bar{E}_{b,2} &= - \frac{d \mathcal{L}_{E_{b,2}}(s)}{ds} \Big|_{s=0} \\
 &= \eta \tau T \pi \lambda_{RF} \mathcal{K}_0 P_{RF} \left(1 + \frac{2}{\alpha - 2} \right) \mathbb{E}_{|f_r|^2} \left[|f_r|^2 \right]
 \end{aligned} \tag{C.3}$$

where $\mathcal{L}_{E_{b,2}}(s)$ is expressed as in (A.1) with $l_0 = 1$. Note that $|f_r|^2 \sim \Gamma(N_E, 1)$, thus $\mathbb{E}_{|f_r|^2} \left[|f_r|^2 \right] = N_E$. Finally, the total average harvested energy is achieved by taking the aggregate of $\bar{E}_{b,1}$ and $\bar{E}_{b,2}$.

REFERENCES

- [1] N. Zhao, F. R. Yu, M. Li, Q. Yan, and V. C. Leung, "Physical layer security issues in interference-alignment-based wireless networks," *IEEE Commun. Mag.*, vol. 54, no. 8, pp. 162–168, Aug. 2016.
- [2] N. Zhao, F. R. Yu, and V. C. Leung, "Wireless energy harvesting in interference alignment networks," *IEEE Commun. Mag.*, vol. 53, no. 6, pp. 72–78, Jun. 2015.
- [3] METIS. *Mobile and Wireless Communications Enablers for the 2020 Information Society*, accessed on Jan. 2015. [Online]. Available: <https://www.metis2020.com>
- [4] C. Yuen, M. Elkashlan, Y. Qian, T. Q. Duong, L. Shu, and F. Schmidt, "Energy harvesting communications: Part 1 [Guest Editorial]," *IEEE Commun. Mag.*, vol. 53, no. 6, pp. 54–55, Jun. 2015.
- [5] C. Yuen, M. Elkashlan, Y. Qian, and T. Q. Duong, "Energy harvesting communications: Part 2 [Guest Editorial]," *IEEE Commun. Mag.*, vol. 53, no. 6, pp. 54–55, Jun. 2015.
- [6] C. Yuen, M. Elkashlan, Y. Qian, T. Q. Duong, L. Shu, and F. Schmidt, "Energy harvesting communications: Part 3 [Guest Editorial]," *IEEE Commun. Mag.*, vol. 53, no. 6, pp. 54–55, Jun. 2015.
- [7] M. L. Ku, W. Li, Y. Chen, and K. J. R. Liu, "Advances in energy harvesting communications: Past, present, and future challenges," *IEEE Commun. Surveys Tuts.*, vol. 18, no. 2, pp. 1384–1412, 2nd. Quart., 2016.
- [8] X. Lu, P. Wang, D. Niyato, D. I. Kim, and Z. Han, "Wireless networks with RF energy harvesting: A contemporary survey," *IEEE Commun. Surveys Tuts.*, vol. 17, no. 2, pp. 757–789, 2nd. Quart., 2015.
- [9] Q. Sun, G. Zhu, C. Shen, X. Li, and Z. Zhong, "Joint beamforming design and time allocation for wireless powered communication networks," *IEEE Commun. Lett.*, vol. 18, no. 10, pp. 1783–1786, Oct. 2014.
- [10] Q. Shi, C. Peng, W. Xu, M. Hong, and Y. Cai, "Energy efficiency optimization for MISO SWIPT systems with Zero-Forcing beamforming," *IEEE Trans. Signal Process.*, vol. 64, no. 4, pp. 842–854, Feb. 2016.
- [11] Q. Shi, L. Liu, W. Xu, and R. Zhang, "Joint transmit beamforming and receive power splitting for MISO SWIPT systems," *IEEE Trans. Wireless Commun.*, vol. 13, no. 6, pp. 3269–3280, Jun. 2014.
- [12] A. A. Nasir, H. D. Tuan, D. T. Ngo, T. Q. Duong, and H. V. Poor, "Beamforming design for wireless information and power transfer systems: Receive power-splitting versus transmit time-switching," *IEEE Trans. Commun.*, vol. 65, no. 2, pp. 876–889, Feb. 2017.
- [13] R. Zhang and C. K. Ho, "MIMO broadcasting for simultaneous wireless information and power transfer," *IEEE Trans. Wireless Commun.*, vol. 12, no. 5, pp. 1989–2001, May 2013.
- [14] K. Huang and E. Larsson, "Simultaneous information and power transfer for broadband wireless systems," *IEEE Trans. Signal Process.*, vol. 61, no. 23, pp. 5972–5986, Dec. 2013.
- [15] K. Huang and V. K. N. Lau, "Enabling wireless power transfer in cellular networks: Architecture, modeling and deployment," *IEEE Trans. Wireless Commun.*, vol. 13, no. 2, pp. 902–912, Feb. 2014.
- [16] C. Zhong, X. Chen, Z. Zhang, and G. K. Karagiannidis, "Wireless-powered communications: Performance analysis and optimization," *IEEE Trans. Commun.*, vol. 63, no. 12, pp. 5178–5190, Dec. 2015.
- [17] Y. Liu, L. Wang, S. A. R. Zaidi, M. Elkashlan, and T. Q. Duong, "Secure D2D communication in large-scale cognitive cellular networks: A wireless power transfer model," *IEEE Trans. Commun.*, vol. 64, no. 1, pp. 329–342, Jan. 2016.
- [18] X. Jiang, C. Zhong, X. Chen, T. Q. Duong, T. A. Tsiftsis, and Z. Zhang, "Secrecy performance of wirelessly powered wiretap channels," *IEEE Trans. Commun.*, vol. 64, no. 9, pp. 3858–3871, Sep. 2016.
- [19] M. Pinuela, P. D. Mitcheson, and S. Lucyszyn, "Ambient RF energy harvesting in urban and semi-urban environments," *IEEE Trans. Microw. Theory Techn.*, vol. 61, no. 7, pp. 2715–2726, Jul. 2013.
- [20] S. Kim *et al.*, "Ambient RF energy-harvesting technologies for self-sustainable standalone wireless sensor platforms," *Proc. IEEE*, vol. 102, no. 11, pp. 1649–1666, Nov. 2014.
- [21] A. H. Sakr and E. Hossain, "Analysis of K -tier uplink cellular networks with ambient RF energy harvesting," *IEEE J. Sel. Areas Commun.*, vol. 33, no. 10, pp. 2226–2238, Oct. 2015.
- [22] Z. Hadzi-Velkov, I. Nikoloska, G. K. Karagiannidis, and T. Q. Duong, "Wireless networks with energy harvesting and power transfer: Joint power and time allocation," *IEEE Signal Process. Lett.*, vol. 23, no. 1, pp. 50–54, Jan. 2016.
- [23] N.-P. Nguyen, T. Q. Duong, H. Q. Ngo, Z. Hadzi-Velkov, and L. Shu, "Secure 5G wireless communications: A joint relay selection and wireless power transfer approach," *IEEE Access*, vol. 4, pp. 3349–3359, 2016.
- [24] Y. Zhu, L. Wang, K. K. Wong, S. Jin, and Z. Zheng, "Wireless power transfer in Massive MIMO-aided HetNets with user association," *IEEE Trans. Commun.*, vol. 64, no. 10, pp. 4181–4195, Oct. 2016.
- [25] S. Akbar, Y. Deng, A. Nallanathan, M. Elkashlan, and A. H. Aghvami, "Simultaneous wireless information and power transfer in K -tier heterogeneous cellular networks," *IEEE Trans. Wireless Commun.*, vol. 15, no. 8, pp. 5804–5818, Aug. 2016.
- [26] Y. Deng, L. Wang, M. Elkashlan, M. D. Renzo, and J. Yuan, "Modeling and analysis of wireless power transfer in heterogeneous cellular networks," *IEEE Trans. Commun.*, vol. 64, no. 12, pp. 5290–5303, Dec. 2016.
- [27] T. A. Khan, A. Alkhateeb, and R. W. Heath, "Millimeter wave energy harvesting," *IEEE Trans. Wireless Commun.*, vol. 15, no. 9, pp. 6048–6062, Sep. 2016.
- [28] X. Jiang, C. Zhong, Z. Zhang, and G. K. Karagiannidis, "Power beacon assisted wiretap channels with jamming," *IEEE Trans. Wireless Commun.*, vol. 15, no. 12, pp. 8353–8367, Dec. 2016.
- [29] Y. Liu, Z. Ding, M. Elkashlan, and H. V. Poor, "Cooperative non-orthogonal multiple access with simultaneous wireless information and power transfer," *IEEE J. Sel. Areas Commun.*, vol. 34, no. 4, pp. 938–953, Apr. 2016.
- [30] M. N. Tehrani, M. Uysal, and H. Yanikomeroglu, "Device-to-device communication in 5G cellular networks: Challenges, solutions, and future directions," *IEEE Commun. Mag.*, vol. 52, no. 5, pp. 86–92, May 2014.
- [31] A. H. Sakr and E. Hossain, "Cognitive and energy harvesting-based D2D communication in cellular networks: Stochastic geometry modeling and analysis," *IEEE Trans. Commun.*, vol. 63, no. 5, pp. 1867–1880, May 2015.
- [32] H. H. Yang, J. Lee, and T. Q. S. Quek, "Heterogeneous cellular network with energy harvesting-based D2D communication," *IEEE Trans. Wireless Commun.*, vol. 15, no. 2, pp. 1406–1419, Feb. 2016.
- [33] S. Shen and R. D. Murch, "Designing dual-port pixel antenna for ambient RF energy harvesting using genetic algorithm," in *Proc. IEEE Int. Symp. Antennas Propag. (USNC/URSI)*, Jul. 2015, pp. 1286–1287.
- [34] C. Song, Y. Huang, J. Zhou, J. Zhang, S. Yuan, and P. Carter, "A high-efficiency broadband rectenna for ambient wireless energy harvesting," *IEEE Trans. Antennas Propag.*, vol. 63, no. 8, pp. 3486–3495, Aug. 2015.
- [35] J. Venkataraman, M. Haenggi, and O. Collins, "Shot noise models for outage and throughput analyses in wireless Ad Hoc networks," in *Proc. IEEE Military Commun. Conf.*, Oct. 2006, pp. 1–7.
- [36] R. A. Horn and C. R. Johnson, *Matrix Analysis*. New York, NY, USA: Cambridge Univ. Press, 1985.
- [37] A. Jeffrey and D. Zwillinger, *Table of Integrals, Series, and Products*. San Diego, CA, USA: Academic, 2007.
- [38] P. A. Digne, R. K. Mallik, and S. S. Jamuar, "Analysis of transmit-receive diversity in Rayleigh fading," *IEEE Trans. Commun.*, vol. 51, no. 4, pp. 694–703, Apr. 2003.
- [39] J. G. Wendel, "The non-absolute convergence of Gil-Pelaez' inversion integral," *Ann. Math. Statist.*, vol. 32, no. 1, pp. 338–339, 1961.



TOAN X. DOAN was born in Binh Du'ong, Vietnam. He received the B.S. degree and the M.S. degree in electronics and telecommunication engineering from the Ho Chi Minh City University of Technology, Vietnam, in 2002 and 2004, respectively. He is currently pursuing the Ph.D. degree with the Queen's University of Belfast. His research interests include energy-harvesting communications and heterogeneous networks.



TIEP M. HOANG was born in Đắk Lắk, Vietnam, in 1989. He received the B.S. degree in electronics and electrical engineering from the HCMC University of Technology, Vietnam, in 2012, and the M.S. degree in electronics and radio engineering from Kyung Hee University, Gyeonggi-do, South Korea, in 2014. He is currently pursuing the Ph.D. degree with the Queen's University of Belfast, Belfast, U.K. In 2015, he was a Research Assistant with Duy Tan University, Danang, Vietnam.



TRUNG Q. DUONG (S'05–M'12–SM'13) received the Ph.D. degree in telecommunications systems from the Blekinge Institute of Technology, Sweden, in 2012. Since 2013, he has been with the Queen's University of Belfast, U.K., as a Lecturer (Assistant Professor). He has authored or co-authored of 240 technical papers published in scientific journals and presented at international conferences. His current research interests include physical layer security, energy-harvesting commu-

nications, and cognitive relay networks. He received the Best Paper Award at the IEEE Vehicular Technology Conference 2013, the IEEE International Conference on Communications 2014, and the IEEE Global Communications. He is a recipient of prestigious Royal Academy of Engineering Research Fellowship from 2016 to 2021. He currently serves as an Editor of the IEEE TRANSACTIONS ON COMMUNICATIONS, the IEEE TRANSACTION ON WIRELESS COMMUNICATIONS, the textitIET Communications and a Senior Editor of the IEEE COMMUNICATIONS LETTERS. He has also served as the Guest Editor of the special issue for the IEEE JOURNAL IN SELECTED AREAS ON COMMUNICATIONS, the textitIET Communications, the textitIEEE Wireless Communications Magazine, the textitIEEE Communications Magazine, the textitEURASIP Journal on Wireless Communications and Networking, the textitEURASIP Journal on Advances Signal Processing, and he was an Editor of the *IEEE Communications Letters*, the *Wiley Transactions on Emerging Telecommunications Technologies*, and the *Electronics Letters*.



HIEN QUOC NGO (S'12) received the B.S. degree in electrical engineering from the Ho Chi Minh City University of Technology, Vietnam, in 2007, the M.S. degree in electronics and radio engineering from Kyung Hee University, South Korea, in 2010, and the Ph.D. degree in communication systems from Linköping University, Sweden, in 2015. In 2014, he visited Bell Laboratories, Murray Hill, NJ, USA. He is currently a Research Fellow with the Division for

Communication Systems, Department of Electrical Engineering, Linköping University. He is also a Visiting Research Fellow with the School of Electronics, Electrical Engineering and Computer Science, Queen's University of Belfast, U.K. His current research interests include massive (large-scale) MIMO systems and cooperative communications. He has been a member of Technical Program Committees for several IEEE conferences, such as ICC, GlobeCom, VTC, WCSP, ISWCS, ATC, and ComManTel. He received the Stephen O. Rice Prize in Communications Theory in 2015, and the IEEE Sweden VT-COM-IT Joint Chapter Best Student Journal Paper Award in 2015. He was an IEEE Communication Letters Exemplary Reviewer for 2014 and an IEEE TRANSACTIONS ON COMMUNICATIONS Exemplary Reviewer for 2015.

• • •